ELSEVIER

Journal of Molecular Catalysis A: Chemical 161 (2000) 171–178

JOURNAL OF MOLECULAR CATALYSIS A: CHEMICAL

www.elsevier.com/locate/molcata

Decomposition of ammonia over a catalyst consisting of ruthenium metal and cerium oxides supported on Y-form zeolite

Keiji Hashimoto *, Naoji Toukai

Osaka Municipal Technical Research Institute, Morinomiya, Joto-ku Osaka, 536-8553 Japan

Received 9 January 2000; received in revised form 2 March 2000; accepted 6 June 2000

Abstract

Ammonia decomposition proceeds at 300°C over a catalyst consisting of ruthenium metal and CeO_2 highly dispersed on Y-form zeolite. The catalyst, Ru-CeO_2/YZ, is highly active for NH_3 decomposition under conditions at which Y-form zeolite and CeO_2 do not work. The decomposition rate is first order in ammonia. The initial rate of nitrogen adsorption supports the decomposition mechanism involving a rate-limiting step in dinitrogen desorption. Moreover, the load of ruthenium particles on CeO_2/YZ catalyst makes an inhibition of the decomposition rate by hydrogen less strong. IR spectra for the catalyst indicate that the ammonia decomposition proceeds via the formation of the intermediate species, such as Ru−NH_3, Ru−NH_2, Ru−N_2 and Ru−H on the surface of ruthenium. The adsorption of hydrogen and XRD data support the idea that ruthenium is highly dispersed in the Ru-CeO_2/YZ

Keywords: Ruthenium metal; Cerium oxides; Y-form zeolite

1. Introduction

Cerium oxides possess unique features, such as stabilization of noble metal dispersion [1–5] and ability to improve hydrogen poisoning [6–8]. This oxide has been used as catalytic support to promote dinitrogen activation or ammonia synthesis [9–11], which is very important as basic chemicals and raw materials for synthetic fertilizer It is, therefore, important to improve the catalytic properties of the oxide. The decomposition and synthesis of ammonia have played important roles in the development of a large number of kinetic principles and so the studies on the decomposition should give a pointer to improve synthetic ammonia catalyst. In addition, the decomposition of ammonia exhausted in the atmosphere is essential to avoid an environmental pollution, for example, ammonia is generated very often on treating sewage and activated sludge. The fine particles of a catalytic material have been frequently used to improve its catalytic properties [12–22]. We have reported that small particles of CeO_2 incorporated into zeolite cavities are highly activated and accelerates the oxidation of alkyl benzene [23]. In this paper, we report (1) preparation of ruthenium

* Corresponding author. Tel.: +81-6-9638031; fax: +81-6-9638040.

E-mail address: hasimoto@omtri.city.osaka.jp (K. Hashimoto).

1381-1169/00/$ - see front matter
PII: S1381-1169(00)00332-0

and CeO_2 highly dispersed in Y-form zeolite, (2) high activity for ammonia decomposition, (3) adsorption species on the surface of ruthenium.

2. Experimental

2.1. Materials

All chemicals were analytical grade commercial materials and used without further purification. The protonated form Y-form zeolite was supplied by the Catalyst Reference Committee of the Japan Catalysis Society. Nitrogen and hydrogen gas (more than 99.9%) were purified according to a usual method, and then dried at 77 K over a molecular sieve (4 Å).

2.2. Preparation of CeO_2 / YZ catalyst

Small particles of cerium oxide supported on Y-form zeolite, CeO_2/YZ, are prepared by the method similar to that reported earlier [23].

2.3. Preparation of Ru-CeO_2 / YZ catalyst

Ruthenium trichloride hydrate (1 g = 0.004 mol) was dissolved in 5 ml of distilled water in a 200 ml beaker and then 10 ml of 85 mol% hydrazine solution was added drop wise carefully at room temperature to the well-stirred ruthenium solution. The solution was stirred for 20 h at room temperature with a magnetic stirrer and then was filtered by a glass filter. The filtered solution contains a mixture of hexaammineruthenium(II) and pentaammine(nitrogen)ruthenium(II) ions [24]. Large quantity of ammonia gas formed by the decomposition of hydrazine was evolved in vacuo. The solution was evaporated in vacuo at 65°C till the volume of the solution became about 2 ml. The evaporation procedures changed the solution from chocolate-brown to wine-red; $[Ru(NH_3)_5(N_2)]^{2+}$ yellow, $[Ru(NH_3)_5Cl]^{2+}$ yellow, $[Ru(NH_3)_5(OH)]^{2+}$ wine-red [24]. The wine-red solution was diluted to 100 ml with distilled water. The CeO_2/YZ (2 g) was placed in 100 ml of the wine-red solution in a 200 ml Erlenmeyer flask. The CeO_2/YZ was impregnated for 12 h at 65°C in the wine-red solution. The impregnation changed the CeO_2/YZ slurry from pale yellow to wine-red. The wine-red slurry was filtered, washed several times with 500 ml of deionized water, and dried at 100°C for 5 h. A dark gray powder was obtained. The dark gray powder was evacuated at 400°C until no ammonia gas was desorbed. The sample changed dark gray to black. The chemical composition of the Ru-CeO_2/YZ was analyzed by inductively coupled plasma (ICP) measurements. The results are summarized in Table 1. The contents of SiO_2, Al_2O_3, CeO_2 and Ru were determined to be 64.0, 19.5, 10.2 and 1.9 wt.%, respectively.

Table 1
Chemical composition

Composition (wt.%)	Ru/CeO_2-YZ
SiO_2	64.0
Al_2O_8	19.5
CeO_2	10.2
Ru	1.9
Na_2O	3.1
Ig. Loss	1.3

2.4. Decomposition of ammonia

The catalyst (0.020 g) was placed in a constant volume of a glass tubular reactor that is connected to a vacuum line and pressure gages (MKS Baratron type 627A11TBC and 622A13TBE). The reactor is a closed system without circulation; the inner diameter of the tubular reactor is 6 mm and reactor volume is 83 ml. The sample was pretreated in vacuo for 3 h at 400°C and then exposed at a fixed temperature to 2–4 kPa of NH_3. The decomposition rate was determined on the basis of a reactor volume and an increase in reaction pressure resulting from ammonia decomposition:

$$2NH_3 \rightarrow N_2 + 3H_2$$

2.5. X-ray measurements

XRD patterns of the samples were recorded using a Mac-Science 18 spectrometer (Ni-Filtered Cu Kα, 40 kV, 50 mA). The samples were mounted on sample boards and the measurements were carried out immediately.

2.6. Chemisorption of nitrogen and hydrogen

The amount of nitrogen chemisorption at 0°C and the rate of nitrogen chemisorption at 300, 330 and 350°C were measured under a desired pressure of nitrogen using a Magnetic Suspension Balance-Low Pressure (Rubotherm Prazisionsmesstechnik Ghbh). The sample was pretreated in vacuo for 2 h at 400°C. The sample was then reduced for 30 min at 300°C with 15 kPa of hydrogen and evacuated for 1 h at 350°C to remove chemisorbed hydrogen and adsorbed water prior to nitrogen adsorption at 0, 300, 330 and 350°C under a desired pressure of nitrogen. The amount of hydrogen chemisorption at 0°C at 1.55 kPa of hydrogen and the rate of hydrogen chemisorption at 300°C at 9 kPa of hydrogen were also measured using the apparatus as described above. The other procedures were the same as described above.

2.7. FTIR measurements

FTIR spectra were recorded on a Shimadzu 8100 FTIR spectrometer using a conventional IR cell connected to a vacuum line and adsorption apparatus. The catalyst (0.001 g) was compressed at 7.5 ton cm^{-2} using a pellet die to form a circular disk with a 3 mm diameter. All samples were pretreated in vacuo for 3 h at 400°C before the FTIR measurements. The sample was exposed at 300°C to NH_3 gas under 0.10 kPa of NH_3. The FTIR measurements were carried out at room temperature.

3. Results and discussion

The decomposition rates of NH_3 were measured at 300, 320, 330 and 350°C under nitrogen pressure of 2–4 kPa and determined using an increase in reaction pressure due to decomposition. The time-on-stream variation in the partial pressure of NH_3 for the decomposition of NH_3 at different temperature is shown in Fig. 1. Y-form zeolite and CeO_2 have no decomposition activity under the conditions. The logarithmic partial pressure of NH_3 falls in proportion to reaction time. The result indicates that the decomposition rate is first order in partial pressure of NH_3 and hydrogen has little effect on the decomposition rate below 320°C. The small deviation at 330 and 350°C from a straight for the reaction time higher than 10 min are additionally due to small variations in the pressure of NH_3 resulting from incomplete diffusion of NH_3 in the slender reaction.

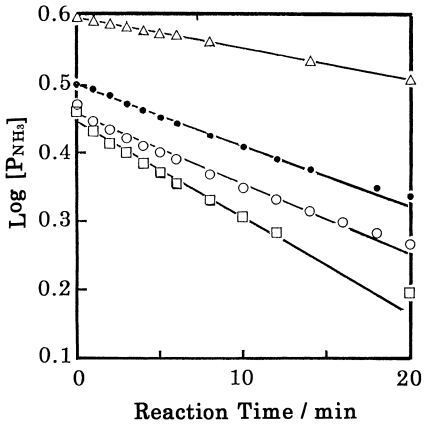

Fig. 1. Variation of partial pressure of NH_3 with reaction time (△) at 300°C,(●) 320°C, (○) 330°C, (□) 350°C; reaction volume: 83.5 ml; catalyst: 17.0 mg.

The initial rates of nitrogen adsorption on the bare surface of the catalyst were measured at 300, 330 and 350°C under nitrogen pressure of 2.0 and 7.0 kPa, and the results were shown in Table 2. The initial rate corresponds to the decomposition rate at the same temperature in Fig. 1. The decomposition rate and initial rate of nitrogen chemisorption are both of the same order of magnitude, 10^{-5} mol min^{-1} g-cat^{-1}. In addition, the equilibrium adsorption of hydrogen was instantaneously attained on introducing hydrogen at 300°C. The initial rate of hydrogen chemisorption on the bare surface is more than 6.0×10^{-3} mol min^{-1} g-cat^{-1} at 9 kPa of hydrogen. These results support the decomposition mechanism involving a rate-limiting step in nitrogen desorption. The ammonia decomposition and its reverse reaction generally involve a rate-limiting step in dinitrogen desorption [25–27]. The decomposition rates (ν_d) under the pressure of ~100 kPa are often fitted by

$$\nu_d = k'\left(P_{NH_3}\right)^n \quad (1a)$$

or

$$\nu_d = \frac{k\left(P_{NH_3}\right)}{\left[1 + K\left(P_{NH_3}\right)\right]} \quad (2a)$$

Table 2
Rate of nitrogen adsorption on Ru/CeO_2-YZ

Adsorption temperature (°C)	Adsorption rate (10^{-5} mol min g-cat^{-1})	
	2.0 kPa	7.0 kPa
300	4.1	9.6
330	9.5	21
350	14	38 (5.5 kPa)

where k, k', K and n $(0 \leqq n \leqq 1)$ are constants [28–32]. In the expressions, (P_{NH_3}) represents a partial pressure of ammonia. Eq. (3a) is derived by substituting $n = 1$ in Eq. (1a) or $1 \gg K(P_{NH_3})$ for denominator term in Eq. (2a).

$$\nu_d = k'(P_{NH_3}) \quad \text{or} \quad \nu_d = k(P_{NH_3})$$

$$\nu_d = k_d(P_{NH_3}) \tag{3a}$$

where k_d is a constant. The reaction is generally zero order in N_2 and H_2, first order in NH_3, and can be inhibited by NH_3 [32]. The observations are reasonably fitted by Eq. (3a). Ammonia synthesis over Ru powder [25] and Ru supported on X-form zeolite [33] is limited by nitrogen adsorption and strongly inhibited by hydrogen; decreasing the H_2 content down to 650 ppm does not suffice to make the inhibition disappear. In the $Ru\text{-}CeO_2/YZ$, little inhibition effect of hydrogen on the rate has been observed as described above. It is reasonably considered that the load of ruthenium particles on CeO_2/YZ significantly makes the inhibition effect by hydrogen less strong. A similar decrease of the inhibition by hydrogen has been reported for the catalytic reaction [8,27,34,35]. The decomposition rate in the $Ru\text{-}CeO_2/YZ$, 5×10^{-2} μmol s^{-1} g-cat^{-1} at 350°C under 2.8 kPa of NH_3, is higher by 100 times than that, 5×10^{-4} μmol s^{-1} g-cat^{-1} at 440°C under 21 kPa of NH_3, in highly active catalyst reported by Oyama [31], because the former decomposition rate is first order in ammonia and the later one is zero order. The Arrhenius plots of the rate constant are represented in Fig. 2 on the basis of the data in Fig. 1. The Arrhenius plots lies near a straight line. The apparent activation energy is determined to be 16 kcal mol^{-1}. The activation energy for dinitrogen adsorption on a variety of supported Ru catalysts, including Ru/Al_2O_3, Ru/MgO, and Ru/CsMgO, ranged from 61 kJ mol^{-1} to 33 kJ mol^{-1} [36]. Assuming the decomposition involving a rate-limiting step in nitrogen desorption, the value (16 kcal mol^{-1}) is reasonable as activation energy for nitrogen desorption, because the value is equal to the sum of the activation energies for nitrogen adsorption and heat of nitrogen adsorption.

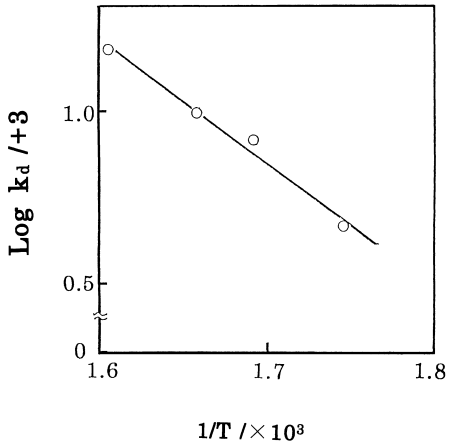

Fig. 2. Arrhenius plots.

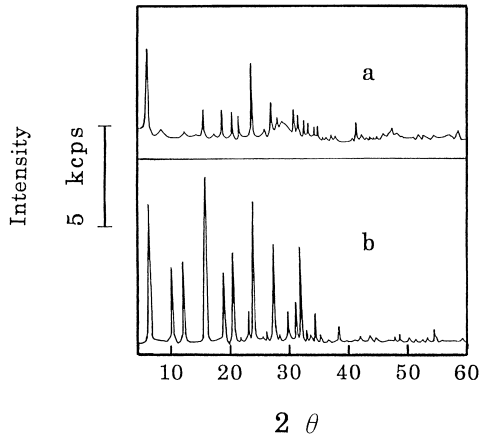

Fig. 3. X-ray diffraction patterns (a) $Ru\text{-}CeO_2$ /YZ; (b) Y-form zeolite.

X-ray diffraction patterns were recorded and shown in Fig. 3. X-ray diffraction patterns for the $Ru\text{-}CeO_2/YZ$ is well in accordance with those for Y-form zeolite [37] except the broad peaks at $2\theta =$ 28.6°, 33.1°, 47 5° and 56.4°. The catalyst maintains the structure of Y-form zeolite. No diffraction pattern resulting from ruthenium metal suggests high

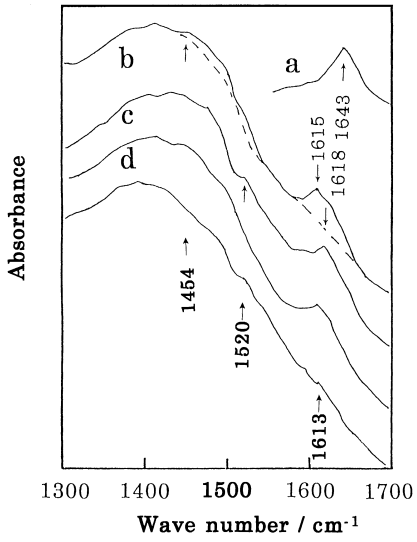

Fig. 4. IR spectra in the range of 1700–1300 cm^{-1}. (a) Y-form zeolite exposed at 300°C to 0.1 kPa of NH_3; (b) Ru-CeO_2 /YZ exposed at 300°C for 10 min to 0.1 kPa of NH_3; (c) Ru-CeO_2 /YZ exposed at 300°C for 40 min to 0.1 kPa of NH_3; (d) Ru-CeO_2 /YZ evacuated at room temperature for 1 min; (e) Ru-CeO_2 /YZ evacuated at 300°C for 10 min; dotted line: back ground.

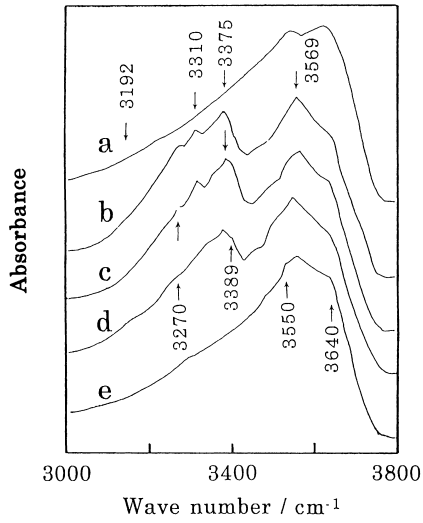

Fig. 5. IR spectra in the range of 3800–3000 cm^{-1}. (a) Evacuation at 400°C for 3 h; (b) Ru-CeO_2 /YZ exposed at 300°C for 10 min to 0.1 kPa of NH_3; (c) Ru-CeO_2 /YZ exposed at 300°C for 40 min to 0.1 kPa of NH_3; (d) Ru-CeO_2 /YZ evacuated at room temperature for 1 min; (e) Ru-CeO_2 /YZ evacuated at 300°C for 10 min.

dispersion of ruthenium in the zeolite. The X-ray diffraction peaks, resulting from a cubic crystal structure of CeO_2, appear in the range of $2\theta = 28.6°$ (III), 33.1° (200), 47 5° (220) and 56.4° (311); their relative intensities are 100, 30, 52 and 42, respectively.[1] We had already reported that small particles of CeO_2 incorporated into the mordenite cavities, CeO_2/Mordenite, were prepared by a hydrolysis of cerium ions with a moist ammonia gas [23]. The CeO_2/YZ was prepared by the same procedures as those of the CeO_2/Mordenite except the use of Y-form zeolite [23]. The broad peaks are attributed to the small crystal size of CeO_2 highly dispersed on Y-form zeolite.

FTIR spectra were measured for the Ru-CeO_2/YZ and shown in Figs. 4–6. As shown in Fig. 4, bands at 1618 ~ 3, 1520 and 1454 cm^{-1} were observed. Coordinated and adsorbed ammonia display the bands, resulting from NH_2 or NH bending, in the region of 1650–1515 cm^{-1}. IR absorption, arising from N—H bending vibration of NH_3 coordinated to ruthenium, occurs in the range of 1634–1605 cm^{-1}

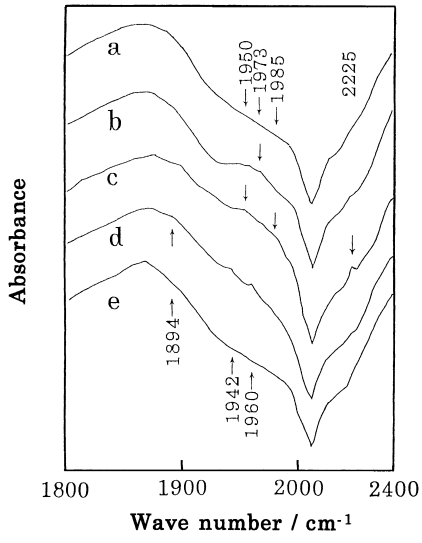

Fig. 6. IR spectra in the range of 2400–1800 cm^{-1}. (a) Evacuation at 400°C for 3 h; (b) Ru-CeO_2 /YZ exposed at 300°C for 10 min to 0.1 kPa of NH_3; (c) Ru-CeO_2 /YZ exposed at 300°C for 40 min to 0.1 kPa of NH_3; (d) Ru-CeO_2 /YZ evacuated at room temperature for 1 min; (e) Ru-CeO_2 /YZ evacuated at 300°C for 10 min.

[1] Powder Diffraction File Inorganic Joint Committee on Powder Diffraction Standards, JCPDS, International Center for Diffraction Data, JCPDS 34-394.

[38], whereas arising from that of NH_3 chemisorbed on Lewis acid sites and Brönsted acid sites, occurs the band at 1620 cm^{-1} and around 1400 cm^{-1}, respectively [39]. On MgO catalyst, the intermediate species of ammonia synthesis, such as NH(a), NH_2(a), and NH_3(a), results in bands at 1410, 1550 and 1610 cm^{-1}, respectively [40]. The band at 1643 cm^{-1} was observed for the Y-form zeolite, but the Y-form zeolite scarcely displays bands in the range of 1600–1200 cm^{-1}. The bands at 1618–3 cm^{-1} can attribute to N—H bending vibration due to ammonia coordinated to ruthenium and/or chemisorbed on Lewis acid sites in the Ru-CeO_2/YZ. The band 1520 cm^{-1} is attributable to the bending vibration of N—H in NH_2 species. The band at 1454 cm^{-1} is attributable to the bending vibration of N—H due to NH_4^+ bonded with Brönsted acid sites, because an increase in decomposition time scarcely influences on the intensity of the band.

As shown in Fig. 5, the bands at 3389, 3375 (with a shoulder at 3337 cm^{-1}), 3310 and 3270 cm^{-1} (with a shoulder 3192 cm^{-1}), were observed on adsorption of NH_3 at 300°C. The stretching vibration of N—H in ruthenium ammine complexes displays the bands around 3100–3375 cm^{-1} [38]. The ruthenium ammine complexes display three bands, resulting from the stretching vibration of NH_3; $[Ru(NH_3)_5N_2]Br$ 3300 cm^{-1} (with a shoulder at about 3230 and 3180 cm^{-1}); $[Ru(NH_3)_5N_2](BF_4)_2$ 3370, 3310, 3230 cm^{-1}; $[Ru(NH_3)_5N_2](PF_6)_2$ 3375, 3306, 3225 cm^{-1} [38]. IR absorption, arising from N—H vibration, gives the bands at 3444, 3337, 1627, around 950 cm^{-1} for NH_3 and 3380, 3290, 1610 cm^{-1} for the adsorption species of NH_2, NH_2(a) and 3200 cm^{-1} for the adsorption species of NH, NH(a) [39,41]. Bands at 3399 cm^{-1} (with a shoulder around 3390 cm^{-1}), 3318 and 3270 cm^{-1} are observed for the Y-form zeolite (Fig. 7). The band at 3375 cm^{-1} with a shoulder around 3340 cm^{-1} and the shoulder at 3192 cm^{-1} appear in the presence of ruthenium and CeO_2. Though IR absorption, arising from the symmetric stretching vibration of NH_3 gas, shows a band at 3337 cm^{-1} [39], the shoulder around 3340 cm^{-1} remains after 1 min evacuation at room temperature. Furthermore, in the FTIR measurements, the bands due to NH_3 in gas phase are canceled out by difference spectrum. Therefore, the bands at 3375 (with a shoulder around 3340 cm^{-1}), about 3310 and 3192 cm^{-1} are attributable to the symmetric stretching vibration of NH_3 coordinated to ruthenium. The increase in decomposition time results in a blue shift of the stretching vibration at 3375 and 3310 cm^{-1}. Furthermore, the evacuation at room temperature results in a red shift of their bands (Fig. 5d). The results indicate the existence of some adsorption species that have a different strength of a bond between their species and adsorption sites. The results are hence explainable in terms of a multiformity in the active sites: ammonia decomposition rapidly and mainly occurs in the more active sites, but slowly in less active ones. The bond strength between NH_2(a) and the more active sites is stronger than that in the less active sites, that is, the electron density of H_2N—Ru bond with the more active sites is higher than that with the less active sites. In the more active sites, the higher density of electron in the H_2N—Ru bond may be attributable to decreasing influence of the electron density of H—N bond. This decrease gives a red shift of stretching vibration of H—N bond. The lower frequency bands due to the intermediate bonded with more active sites, thus, are observed in the initial reaction stage and at an evacuation, whereas the rather high frequency one due to the intermediate on less active sites is observed after a long reaction time. Therefore, the difference between the more active and less active sites is believed to be due to different location of ruthenium particles in the inner and on the outer surface of the zeolite.

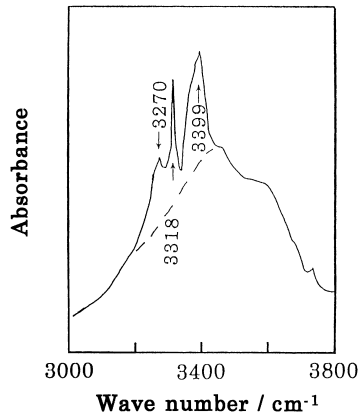

Fig. 7. IR spectra of ammonia species adsorbed on Y-form zeolite Adsorption at 300°C under pressure with 0.1 kPa of NH_3.

The bands at ca. 2225, 1985, 1973, 1960, 1950 and 1894 cm^{-1} were observed for the Ru-CeO_2/YZ (Fig. 6), whereas these bands were not recognized for Y-form zeolite which is inactive for the decomposition. IR absorption, arising from the stretching vibration of Ru—H, shows bands in the range of 2000–1880 cm^{-1}, resulting from on-top, and side-on type adsorption [42–44]. IR absorption, arising from the stretching frequency of dinitrogen molecules adsorbed on ruthenium, bands in the range of 2240–2020 cm^{-1} [11,42,45]. The intensity of the band around 2225 cm^{-1} decreases on evacuation at room temperature for 1 min, and the band simultaneously shifts to lower frequency. The band around 2225 cm^{-1} is attributed to the stretching vibration of dinitrogen molecules formed by the decomposition of ammonia. A similar shift, resulting from the adsorption of nitrogen on the multiform active sites, has been observed for the stretching vibration of N≡N bonding with ruthenium [11,46]. The bands at 1985, 1973, 1960, 1950 and 1894 cm^{-1} are attributed to the stretching frequency of Ru—H in the on-top type adsorption. The intensities of the bands increase with an increase in decomposition time (Fig. 6b and c). The evacuation at room temperature results in a decrease of the intensity of the bands due to Ru—H (Fig. 6d). The band at 1942 and 1960 cm^{-1} remain after the evacuation. The results are explainable in terms of the same explanation of frequency shift at 3375 and 3310 cm^{-1} as described above: ammonia decomposition rapidly occurs in the more active sites, but slowly in less active ones. The hydrogen species strongly bonded with the more active sites may give the lower frequency bands, because the adsorption ability of the active sites depends on a shift quantity from 2000 cm^{-1} [42,43]. These results substantiate the proposal that the active sites in the Ru-CeO_2/YZ have certain multiformity. A similar shift due to a multiformity in the active sites has been observed for the stretching vibration of Ru—H in the ruthenium catalysts [42,43].

The amount of nitrogen chemisorption was measured at 0°C under 3.25 kPa of nitrogen and was determined to be 1.6×10^{-5} mol g-cat^{-1}. Similarly, the amount of hydrogen chemisorption was measured at 0°C under 1.55 kPa of hydrogen. The amount is determined to be 4.2×10^{-5} mol g-cat^{-1} at 0°C even under 1.55 kPa of hydrogen which is half a pressure of nitrogen. No hydrogen is chemisorbed on the CeO_2/YZ under the same conditions. On the other hand, the amount of the supported ruthenium is calculated to be 1.8×10^{-4} mol g-$cat^{-1} = 0.019/101.007$ from the chemical composition in Table 1 and an atomic mass of ruthenium. Assuming that hydrogen atom bonds with one ruthenium atom and hydrogen coverage is 100%, the number of the adsorption sites of dissociative hydrogen possesses $46\% = (4.2 \times 10^{-5}) \times 2 \times 100/1.8 \times 10^{4}$ of the amount of the supported ruthenium, that is, the number of surface ruthenium atoms is 5.1×10^{17} atoms g-$cat^{-1} = 4.2 \times 10^{-5} \times 2 \times 6.02/10^{23}$. The former value, 46%, indicates that the ratio of surface Ru atoms to bulky Ru atoms is 46/54. The average size of Ru particles is calculated to be ca. 2 nm on the basis of the ratio, closest packing and atomic radius of Ru. Similarly, the number of nitrogen adsorption sites at 0°C under 3.25 kPa of nitrogen possess $9\% = (1.6 \times 10^{-5}) \times 100/1.8 \times 10^{-4}$ of the amount of the supported ruthenium. The difference between the amount of hydrogen- and nitrogen-adsorption is probably due to lower nitrogen coverage under the conditions. The results indicate that small particles of ruthenium are highly dispersed in the CeO_2/YZ.

4. Conclusion

The catalyst consisting of ruthenium and CeO_2 highly dispersed on Y-form zeolite have been prepared. The Ru-CeO_2/YZ is highly active for NH_3 decomposition under the conditions at which Y-form zeolite and CeO_2 don't work. The decomposition rate is first order in ammonia and hydrogen has little effect on the decomposition rate below 320°C. The initial rate of nitrogen chemisorption on the bare surface corresponds to the decomposition rate at the same temperature. The initial chemisorption rate and decomposition one are both of the same order of magnitude, 10^{-5} mol min^{-1} g-cat^{-1}, whereas the initial rate of hydrogen chemisorption on the bare surface is far faster than the decomposition one. The results support the decomposition mechanism involving a rate-limiting step in nitrogen desorption. The load of ruthenium particles on the CeO_2/YZ makes the inhibition by hydrogen less strong. The observa-

tions are reasonably fitted by Eq. (3a) derived by substituting $n = 1$ in Eq. (1a) or $1 \gg K(P_{NH_3})$ for denominator term in Eq. (2a). The apparent activation energy is determined to be $16\,kcal\,mol^{-1}$. Assuming the decomposition involving a rate-limiting step in nitrogen desorption, the value ($16\,kcal\,mol^{-1}$) is reasonable as activation energy for nitrogen desorption. The adsorption of NH_3 gives the band at $1520\,cm^{-1}$ which is attributable to the bending vibration of N—H in NH_2 species. In addition, the adsorption gives the band at $2225\,cm^{-1}$ and the bands at 1985, 1973, 1960, 1950 and $1894\,cm^{-1}$: the former band is attributable to the stretching vibration of N≡N bonding with ruthenium and the later ones are attributed to the stretching frequency of Ru—H in the on-top type adsorption. These results indicate that the decomposition of NH_3 at 300°C proceeds via a generation of Ru—NH_2, Ru—H and Ru—N_2 species. The ammonia decomposition hence occurs on the ruthenium surface. The adsorption of hydrogen and XRD data support the idea that small particles of ruthenium are highly dispersed in the Ru-CeO_2/YZ.

References

[1] A. Guerrero-Ruiz, A. Sepúlveda-Escribano, I. Rodriguez-Ramos, Appl. Catal. A Gen. 120 (1994) 71.
[2] I.H. Diagne, J.P. Hindermann, A. Kiennemann, Appl. Catal. 51 (1989) 165.
[3] J.C. Lavalley, J. Saussey, J. Lamotte, R. Breault, P. Hindermann, A. Kiennemann, J. Phys. Chem. 94 (1990) 5941.
[4] M.L. Turner, P.K. Byers, P.M. Maitlis, Catal. Lett. 26 (1994) 55.
[5] L.A. Bruce, M.J. Hoang, A.E. Hughes, T.W. Turney, J. Catal. 178 (1998) 84.
[6] S. Murata, K. Aika, J. Catal. 136 (1992) 118.
[7] A. Trovarell, Catal. Rev. Sci. Eng. 38 (1996) 439.
[8] Y. Niwa, K. Aika, J. Catal. 162 (1996) 138.
[9] Y. Izumi, Y. Iwata, K. Aika, J. Phys. Chem. 100 (1996) 9421.
[10] G. Ranga rao, Y. Kadowaki, H. Kondoh, H. Hozoey, Surf. Sci. 327 (1995) 293.
[11] J. Kubota, K. Aika, J. Phys. Chem. 98 (1994) 11293.
[12] P.V. Menacherry, G.L. Haller, J. Catal. 177 (1998) 175.
[13] C. Descorme, P. Gélin, C. Lécuyer, M. Primet, J. Catal. 177 (1998) 352.
[14] L.A. Bruce, M. Hoang, A.E. Hughes, T.W. Turney, J. Catal. 178 (1998) 84.
[15] C. Morterra, E. Giamello, G. Cerrato, G. Centi, S. Parathoner, J. Catal. 179 (1998) 111.
[16] M.A. Cambor, A. Corma, A. Martinez, V. Martinez-Soria, S. Valencia, J. Catal. 179 (1998) 537.
[17] Y. Jiang, S. Decker, C. Mohs, K.J. Kiaubunde, J. Catal. 180 (1998) 24.
[18] W.A. Weber, B.C. Gates, J. Catal. 180 (1998) 207.
[19] J.-D. Grunwaldt, C. Kiener, C. Wögerbauer, A. Baiker, J. Catal. 181 (1999) 223.
[20] T. Bécue, F.T. Maldonado-Hodar, A.P. Antunes, J.M. Silva, M.F. Ribeiro, P. Massiani, M. Kermarec, J. Catal. 181 (1999) 244.
[21] K. Hashimoto, N. Toukai, J. Mol. Catal. A Chem. 138 (1999) 59.
[22] K. Hashimoto, N. Toukai, Appl. Catal. A Gen. 180 (1999) 367.
[23] K. Hashimoto, K. Matzuo, H. Kominami, Y. Kera, J. Chem. Soc., Faraday Trans. 93 (20) (1997) 3729.
[24] P.W. Parry, Inorganic Synthesis, Vol. XII, McGraw-Hill, New York, 1970, p. 5.
[25] G. Rambeau, H. Amarigho, J. Catal. 72 (1981) 1.
[26] K. Tanaka, J. Res. Inst. Catal. Hokkaido Univ. 19 (1971) 63.
[27] A. Ozaki, K. Aika, in: J.R. Anderson, M. Boudart (Eds.), Catalysis-Science and Technology, Springer, Berlin, 1981, p. 87.
[28] D.G. Löffler, L.D. Schmidt, J. Catal. 44 (1976) 244.
[29] H. Shindo, C. Egawa, T. Inishi, K. Tamura, J. Chem. Soc., Faraday Trans. 1 76 (1980) 280.
[30] M. Boudart, C. Egawa, S.T. Oyama, J. Chem. Phys. 78 (1981) 987.
[31] S.T. Oyama, J. Catal. 133 (1992) 358.
[32] R.S. Wise, E.J. Markel, J. Catal. 145 (1994) 335.
[33] T. Bécue, R.J. Davis, J.M. Carces, J. Catal. 179 (1998) 129.
[34] S.R. Tennison, in: J.R. Jennings (Ed.), Catalytic Ammonia Synthesis, Plenum Press, New York, 1991, p. 303.
[35] K. Aika, K. Tamaru, in: A. Nielsen (Ed.), Ammonia Catalysis and Manufacture, Springer, Berlin, p. 103.
[36] O. Hinrichsen, F. Rosowski, A. Hornung, M. Muhler, G. Ertl, J. Catal. 165 (1997) 33.
[37] H. Tominaga, Zeolite no Kagaku to Ouyo, Kondansya Scientific, 1990, p. 24.
[38] A.D. Allen, F. Bottomley, R.O. Harris, V.P. Reinsalu, C.V. Senoff, J. Am. Chem. Soc. 89 (1967) 5595.
[39] K. Nakamoto, Infrared and Raman Spectra of Inorganic and Coordination Compounds, Wiley, New York, 1986.
[40] S. Kagami, T. Onishi, K. Tamaru, J. Chem. Soc., Faraday Trans. 1 80 (1983) 29.
[41] T. Nakata, S. Matsushima, J. Phys. Chem. 72 (1968) 458.
[42] Y. Izumi, A. Aika, J. Phys. Chem. 99 (1995) 10346.
[43] Y. Izumi, M. Hoshikawa, K. Aika, Bull. Chem. Soc. Jpn. 67 (1994) 3191.
[44] H.D. Kaes, R.B. Saillant, Chem. Rev. 72 (1972) 231.
[45] B.C. Lyutov, Y.G. Borodko, Kinet. Katal. 12 (1971) 1566.
[46] M. Oh-kita, K. Aika, K. Urabe, A. Ozaki, J. Catal. 44 (1976) 460.